

# Clathrin-Dependent and Clathrin-Independent Retrieval of Synaptic Vesicles in Retinal Bipolar Cells

Wolf J. Jockusch, Gerrit J.K. Praefcke, Harvey T. McMahon,\* and Leon Lagnado\*  
Medical Research Council  
Laboratory of Molecular Biology  
Hills Road, Cambridge CB2 2QH  
United Kingdom

## Summary

Synaptic vesicles can be retrieved rapidly or slowly, but the molecular basis of these kinetic differences has not been defined. We now show that substantially different sets of molecules mediate fast and slow endocytosis in the synaptic terminal of retinal bipolar cells. Capacitance measurements of membrane retrieval were made in terminals in which peptides and protein domains were introduced to disrupt known interactions of clathrin, the AP2 adaptor complex, and amphiphysin. All these manipulations caused a selective inhibition of the slow phase of membrane retrieval (time constant  $\sim 10$  s), leaving the fast phase ( $\sim 1$  s) intact. Slow endocytosis after strong stimulation was therefore dependent on the formation of clathrin-coated membrane. Fast endocytosis occurring after weaker stimuli retrieves vesicle membrane in a clathrin-independent manner. All compensatory endocytosis required GTP hydrolysis, but only a subset of released vesicles were primed for fast, clathrin-independent endocytosis.

## Introduction

Synaptic vesicles at the nerve terminal are efficiently recycled following exocytosis, but the mechanisms are still a matter of debate. Using electron microscopy, Heuser and Reese (1973) found that high-frequency stimulation of the frog neuromuscular junction led to depletion of synaptic vesicles and the appearance of coated vesicles at sites removed from the active zone. In contrast, Ceccarelli et al. (1973) found that low-frequency stimuli did not cause depletion of vesicles or formation of coated intermediates and suggested that vesicles were retrieved rapidly at sites of fusion. We now know that the electron-dense coats around vesicles are formed by clathrin, which acts as an organizer of a number of adaptor and accessory proteins (for reviews, see Cremona and De Camilli, 1997; Marsh and McMahon, 1999; Morgan et al., 2002; Royle and Lagnado, 2003). The fast mechanism of endocytosis has proven harder to characterize; it is often thought to occur by the transient opening of a vesicle to the external medium *without* full collapse into the surface mem-

brane, a model termed “kiss-and-run” (reviewed by Jarrousse and Kelly, 2001; Morgan et al., 2002).

The speed of endocytosis at the synapse was first measured directly by applying the capacitance technique to the large synaptic terminal of retinal bipolar cells, where it was found that a brief stimulus was followed by retrieval of excess membrane with a time constant of  $\sim 1$  s (von Gersdorff and Matthews, 1994). After stronger stimulation, fast endocytosis was followed by a slow phase of retrieval with a time constant of  $\sim 10$  s, leading to the suggestion that there were two distinct endocytic processes (Neves and Lagnado, 1999). Exocytosis by “kiss-and-run” does not appear to be a significant mechanism in bipolar cells, because the great majority of fusion events are followed by merging of the vesicle with the plasma membrane (Zenisek et al., 2002) then collapse of the vesicle to cause expansion of the cell surface (Llobet et al., 2003). In addition, fast and slow phases of endocytosis both involve retrieval of collapsed membrane from the surface (Llobet et al., 2003). Intriguingly, it has been suggested that endocytosis at this synapse operates without GTP hydrolysis (Heidelberger, 2001). This idea would appear to rule out clathrin-mediated endocytosis (CME) as a mechanism of vesicle retrieval in bipolar cells, because the GTPase dynamin plays an essential role in CME in a wide range of cell types (Marks et al., 2001). Dynamin also operates during endocytosis at other synapses (Koenig and Ikeda, 1989; Yamashita et al., 2005).

Fast and slow modes of endocytosis have been shown to operate at a number of synapses, including inner hair cells (Beutner et al., 2001), the calyx of Held (Sun et al., 2002), and hippocampal boutons (Gandhi and Stevens, 2003; Klingauf et al., 1998; Pyle et al., 2000; Sankaranarayanan and Ryan, 2000). We now need to bridge the gap between our understanding of kinetics and molecules (Royle and Lagnado, 2003). Do fast and slow endocytosis at the synapse utilize different proteins, or might both occur by a clathrin-dependent mechanism? Under which conditions does CME operate and how rapidly? To investigate these questions, it is necessary to manipulate molecular events at a synapse in which endocytosis can be measured directly. We have therefore used the capacitance technique to make real-time measurements of endocytosis in the synaptic terminal of retinal bipolar cells in which peptides and protein domains were introduced to disrupt known interactions of clathrin, the adaptor complex, and accessory proteins such as amphiphysin. All these manipulations caused a selective inhibition of the slow phase of endocytosis, leaving the fast phase intact. We therefore attribute slow endocytosis, which predominates after stronger stimulation, to the formation of clathrin-coated vesicles. Fast endocytosis occurs by the retrieval of membrane that has collapsed into the surface, but *without* formation of a clathrin coat. The fast and slow modes of endocytosis were both dependent on GTP hydrolysis.

\*Correspondence: hmm@mrc-lmb.cam.ac.uk (H.T.M.); ll1@mrc-lmb.cam.ac.uk (L.L.)

## Results

### GTP Hydrolysis Was Essential for Both Fast and Slow Modes of Endocytosis

A key event in vesicle formation is membrane scission to free the nascent vesicle from the parent membrane. In many trafficking pathways, including CME, this is achieved with the aid of dynamin, a GTPase that constricts membrane (Marks et al., 2001; Sweitzer and Hinshaw, 1998). Recently, it has been suggested that membrane scission in retinal bipolar cells involves hydrolysis of ATP rather than GTP (Heidelberger, 2001). If this were correct, it would argue against a role for dynamin and CME at this synapse. We therefore began this study by reinvestigating the role of GTP hydrolysis during endocytosis in bipolar cells. Figure 1A shows that, after a depolarization lasting 100 ms, there was an increase in the capacitance of the surface membrane, reflecting exocytosis, followed by a decrease, reflecting endocytosis. In terminals dialyzed with our standard internal solution (1 mM GTP and 3 mM ATP), the fall in surface area was best described as the sum of two exponentials with about 40% of the membrane retrieved with a rate constant of  $1.0 \text{ s}^{-1}$  ( $k_{\text{fast}} = 1/\tau_{\text{fast}}$ ), and the remainder with a rate constant of about  $0.1 \text{ s}^{-1}$  ( $k_{\text{slow}}$ ). These rates of fast and slow endocytosis are similar to previous measurements in bipolar cells (Neves and Lagnado, 1999; Hull and von Gersdorff, 2004).

The normalized responses in Figure 1A show that both fast and slow phases of endocytosis were blocked by replacing GTP in the internal solution with a non-hydrolysable analog, GTP- $\gamma$ -S. At a concentration of 5 mM, GTP- $\gamma$ -S was equally effective at blocking membrane retrieval when it was applied in the presence of 3 mM ATP (Figure 1A) or 0.5 mM ATP (Figure 1B). A second way to inhibit the activity of GTPases is to apply GDP- $\beta$ -S (Bloom et al., 1993), and this maneuver also blocked endocytosis (Figure 1C). These results demonstrate that the fast and slow modes of endocytosis in the synaptic terminal of bipolar cells were both dependent on GTP hydrolysis, indicating a key role for dynamin or other GTPases. Recent measurements in the calyx of Held demonstrate that a slow mode of endocytosis in this terminal ( $\tau = 10\text{--}25 \text{ s}$ ) also requires GTP hydrolysis (Yamashita et al., 2005). We could not find any evidence that membrane scission in bipolar cells required ATP hydrolysis; the time course of endocytosis in 0.5 mM ATP was very similar to that observed in 3 mM ATP, and ATP could not substitute for GTP in allowing endocytosis to proceed (Figures 1B and 1C).

### Proteins Binding the Proline-Rich Domain of Dynamin Were Involved in Slow Endocytosis

Dynamin interacts with several recruitment proteins through a proline-rich domain that allows it to function in multiple forms of endocytosis (for reviews, see Praefcke and McMahon, 2004; Schmid et al., 1998). One such protein is amphiphysin, which contains an SH3 domain that binds a PxRPxR sequence in mammalian dynamins (Grabs et al., 1997; Owen et al., 1998) and is enriched in nerve terminals (David et al., 1996; Shupliakov et al., 1997; Wigge et al., 1997). A peptide incorporating the PxRPxR sequence inhibits CME at the lamprey giant reticulospinal synapse (Shupliakov et

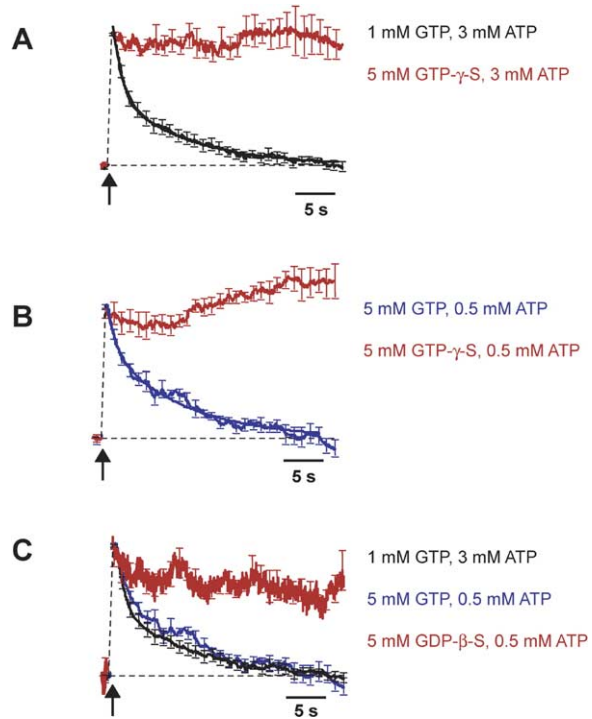


Figure 1. Fast Endocytosis and Slow Endocytosis in Bipolar Cells Were Both Dependent on GTP Hydrolysis

(A) Normalized capacitance responses elicited by a depolarizing step from  $-70 \text{ mV}$  to  $-10 \text{ mV}$  lasting 100 ms (delivered at arrow). Superimposed are averaged responses from terminals dialyzed with standard internal solution (1 mM GTP, 3 mM ATP; black;  $n = 16$ ) and a solution in which GTP was replaced by 5 mM GTP- $\gamma$ -S (red;  $n = 4$ ). The solid trace describing the time courses of endocytosis in standard solution is a double exponential with  $\tau_{\text{fast}} = 1.0 \text{ s}$  and  $\tau_{\text{slow}} = 9.5 \text{ s}$  and 40% of the excess membrane retrieved rapidly. Replacing GTP with GTP- $\gamma$ -S did not significantly alter the amplitude of the  $\text{Ca}^{2+}$  current or the size of the exocytic response. (B) Normalized responses from terminals dialyzed with 5 mM GTP and 0.5 mM ATP (blue;  $n = 6$ ) and 5 mM GTP- $\gamma$ -S and 0.5 mM ATP (red;  $n = 5$ ). The solid trace describing the time courses of endocytosis in standard solution is a double exponential with  $\tau_{\text{fast}} = 1.0 \text{ s}$  and  $\tau_{\text{slow}} = 10.0 \text{ s}$  and 49% of the excess membrane retrieved rapidly. (C) Normalized responses from terminals dialyzed with 5 mM GDP- $\beta$ -S and 0.5 mM ATP (red;  $n = 7$ ), 5 mM GTP and 0.5 mM ATP (blue; from [B]), and 1 mM GTP and 3 mM ATP (black; from [A]). The averaged amplitudes of the capacitance responses and calcium currents were as follows: standard internal solution,  $78 \pm 7 \text{ fF}$  and  $225 \pm 26 \text{ pA}$ ; 5 mM GTP- $\gamma$ -S and 3 mM ATP,  $71 \pm 16 \text{ fF}$  and  $233 \pm 18 \text{ pA}$ ; 5 mM GTP and 0.5 mM ATP,  $48 \pm 9 \text{ fF}$  and  $286 \pm 31 \text{ pA}$ ; 5 mM GTP- $\gamma$ -S and 0.5 mM ATP,  $40 \pm 8 \text{ fF}$  and  $223 \pm 40 \text{ pA}$ ; 5 mM GDP- $\beta$ -S and 0.5 mM ATP,  $83 \pm 9 \text{ fF}$  and  $173 \pm 24 \text{ pA}$ . Error bars in graphs show  $\pm$  one SEM.

al., 1997) and completely blocks a slow mode of endocytosis at the calyx of Held (Yamashita et al., 2005). To investigate the potential role of the dynamin-amphiphysin interaction during endocytosis in retinal bipolar cells, we began by testing whether the proline-rich domain of mammalian dynamin could be used to inhibit the interaction between proteins from the brain of goldfish.

GST-tagged rat amphiphysin 2 SH3 domain (GST-amph-SH3D) was bound to GSH-Sepharose and incubated with extracts from the brains of goldfish or rats.

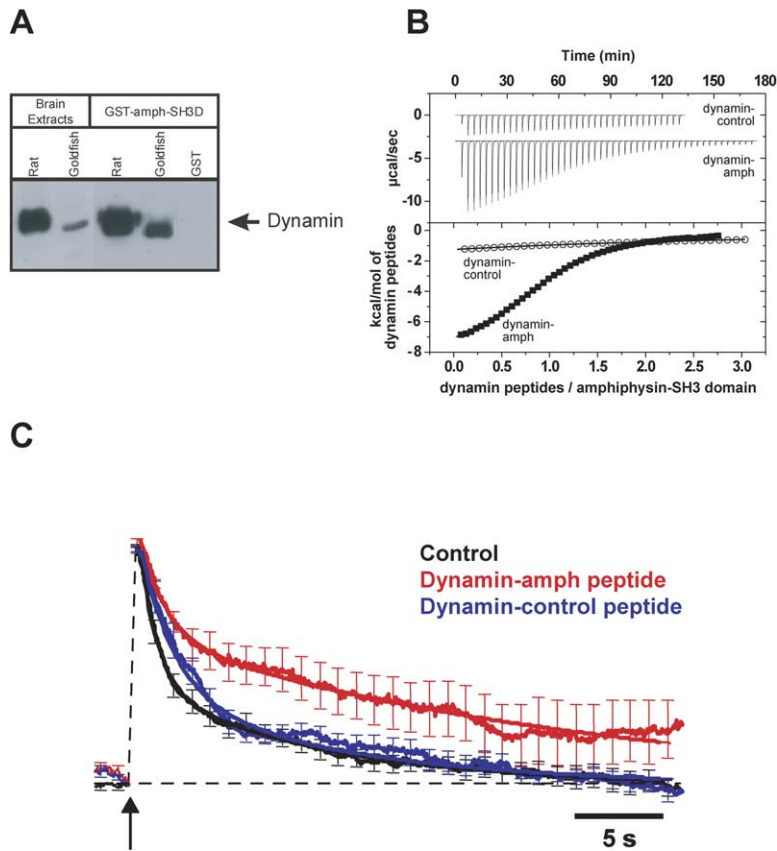


Figure 2. The Slow Mode of Endocytosis Involves an Interaction between Amphiphysin and Dynamin

(A) The interaction between GST-tagged rat amphiphysin 2 SH3 domain (GST-amph-SH3D) and rat or goldfish dynamin was probed using a protein binding assay and followed by immunoblotting.

(B) The interaction between dynamin-derived peptides and the rat amphiphysin 2 SH3 domain was followed by isothermal titration calorimetry. The upper panel shows the heat of binding measured by stepwise injection of 4.25 mM of an amphiphysin binding peptide from dynamin (dynamamin-amph) and 6 mM of a control peptide (dynamamin-control) into 298  $\mu$ M (dynamamin-amph) or 450  $\mu$ M (dynamamin-control) of the amphiphysin-SH3 domain at 10°C. The lower panel shows the integrated heating powers of the upper panel normalized to the concentration of the dynamin peptides.

(C) Normalized capacitance responses elicited by a depolarization lasting 100 ms (delivered at arrow). Averaged responses from terminals dialyzed with standard internal solution (black trace;  $n = 18$ ;  $\tau_{fast} = 1.1$  s and  $\tau_{slow} = 11.4$  s), 1.0 mM dynamamin-amph peptide (red;  $n = 7$ ;  $\tau_{fast} = 1.4$  s and  $\tau_{slow} = 27.8$  s), or 1.0 mM dynamamin-control peptide (blue;  $n = 7$ ;  $\tau_{fast} = 1.9$  s and  $\tau_{slow} = 10.9$  s). Error bars show  $\pm$  one SEM.

The samples were run on a gel and probed by immunoblotting with an anti-dynamin antibody. Goldfish dynamin was detected by the mammalian dynamin antibody, and it bound to rat amphiphysin 2 SH3 domain (Figure 2A). Next, we used isothermal titration calorimetry (ITC) to determine the affinity of a dynamamin-amph peptide (QVPSRPNRAP) for the amphiphysin SH3 domain (Figure 2B). The  $K_D$  was  $90 \pm 19 \mu$ M (average of six independent measurements), indicating that 1 mM of the peptide would be sufficient to inhibit the interaction in a cell. A “dynamamin-control” peptide similarly rich in proline but lacking the PxRPxR sequence (PAVP-PPRPG) had a much lower affinity for the SH3 domain ( $K_D > 1$  mM; Figure 2B).

Each peptide was added to the patch pipette at a concentration of 1 mM, and capacitance changes were measured in response to a depolarization lasting 100 ms. Averaged responses are shown in Figure 2C, together with fits to double exponential functions. The dynamamin-amph peptide inhibited the slow phase of endocytosis by a factor of 3 on average ( $k_{slow} = 0.03 \pm 0.008$  s $^{-1}$  compared to  $0.09 \pm 0.007$  s $^{-1}$  in controls; see Table 1). In contrast, the fast phase of endocytosis was not significantly affected, either in rate ( $k_{fast} = 0.8 \pm 0.23$  s $^{-1}$  compared to  $1.0 \pm 0.14$  s $^{-1}$  in controls) or in amplitude ( $A_{fast} = 50\% \pm 10\%$  compared to  $65\% \pm 5\%$  in controls). The dynamamin-control peptide did not significantly affect the fast or slow phases of endocytosis ( $k_{fast} = 0.7 \pm 0.11$  s $^{-1}$  and  $k_{slow} = 0.10 \pm 0.015$  s $^{-1}$ ). These results support the suggestion that the fast and slow

phases of recovery observed in capacitance records represent mechanisms of endocytosis that utilize different molecules (Neves and Lagnado, 1999; Neves et al., 2001). Although both fast and slow endocytosis required GTP hydrolysis (Figure 1), slow endocytosis also involved proteins binding the PxRPxR sequence in dynamin (Figure 2).

#### Accessory Proteins Containing Clathrin Binding Motifs Were Involved in Slow Endocytosis

Dynamin is involved in many forms of endocytosis, but CME is the best characterized. Clathrin contains a  $\beta$ -propeller domain that interacts with a number of accessory proteins containing “clathrin binding motifs,” including amphiphysin, AP180, and epsin (Dell’Angelica et al., 1998; Krupnick et al., 1997; Ramjaun and McPherson, 1998). We therefore introduced the  $\beta$ -propeller domain of clathrin as a nonselective method of inhibiting interactions of accessory proteins containing clathrin binding motifs. Averaged capacitance responses to a depolarization lasting 100 ms are shown in Figure 3A. Dialysis of terminals with 0.1 mM of the  $\beta$ -propeller domain significantly inhibited the slow phase of endocytosis ( $k_{slow} = 0.03 \pm 0.011$  s $^{-1}$ ) but left the fast phase almost unchanged ( $k_{fast} = 0.9 \pm 0.13$  s $^{-1}$ ; Table 1).

Endocytosis was also slowed by the  $\beta$ -propeller domain of clathrin after a longer stimulus lasting 2 s (Figure 3B). Often, a fast phase of endocytosis was not apparent after this strong stimulus, and recovery of the averaged capacitance response could not be de-

Table 1. Capacitance Responses under Various Experimental Conditions

	$A_{fast}$ (%)	$k_{fast}$ ( $s^{-1}$ )	$k_{slow}$ ( $s^{-1}$ )	$\Delta C_m$ (fF)	$I$ (pA)
Control (n = 18)	65 ± 5	1.0 ± 0.14	0.09 ± 0.007	78 ± 7	225 ± 26
Dynamin-amph (n = 7)	50 ± 10	0.8 ± 0.23	0.03 ± 0.008*	61 ± 7	249 ± 46
Dynamin-control (n = 7)	67 ± 8	0.7 ± 0.11	0.10 ± 0.015	61 ± 6	167 ± 16
Clathrin $\beta$ -propeller (n = 10)	50 ± 9	0.9 ± 0.13	0.03 ± 0.011*	62 ± 7	196 ± 35
Amph1-md mut (n = 10)	59 ± 10	0.8 ± 0.13	0.02 ± 0.008*	108 ± 22	292 ± 46
DNF-12mer (n = 7)	56 ± 5	0.9 ± 0.19	0.02 ± 0.011*	58 ± 6	216 ± 43
DPF-12mer (n = 13)	61 ± 6	1.9 ± 0.22	0.08 ± 0.008	60 ± 11	238 ± 45

$A_{fast}$  is the percentage of the excess membrane retrieved during the fast phase of endocytosis; the remainder was retrieved slowly. The rate constants of the fast and slow phases are  $k_{fast}$  ( $= 1/\tau_{fast}$ ) and  $k_{slow}$  ( $= 1/\tau_{slow}$ ), obtained from  $n$  responses to a 100 ms depolarization (see [Experimental Procedures](#)).  $\Delta C_m$  is the amplitude of the capacitance response to this stimulus, and  $I$  is the amplitude of the calcium current. Errors are one SEM. Asterisks indicate a parameter that differs significantly from its value under control conditions ( $p < 0.05$ ).

scribed as the sum of declining exponentials. We therefore characterized the rate of endocytosis by the time to half-recovery:  $t_{1/2}$  was  $23.0 \pm 1$  s in the presence of 0.1 mM of the  $\beta$ -propeller domain of clathrin, compared to  $10 \pm 1.5$  s in controls. These results demonstrate that slow endocytosis involved proteins containing clathrin binding motifs (such as amphiphysin, AP180, or epsins) and is therefore likely to occur via the formation of clathrin-coated vesicles. Equally, the fast phase of

membrane retrieval did not involve these accessory proteins.

### Clathrin Was Involved in Slow Endocytosis

Dialysis of terminals with the  $\beta$ -propeller domain of clathrin is likely to sequester a number of proteins containing clathrin binding motifs. To assess the role of clathrin more specifically, we used the clathrin binding region from one of these accessory proteins to sequester clathrin itself. The amphiphysin 1 motif domain (amph1-md, residues 318–390) contains two different clathrin binding regions ([Ramjaun and McPherson, 1998](#)), as well as an adaptor binding sequence. To reduce adaptor binding, a point mutation was made in the adaptor binding sequence (FEDNF mutated to FEDAF, amph1-md mut). The specificity of the interaction between this peptide and goldfish clathrin was tested by adding extracts of rat and goldfish brain to GST-coupled amph1-md mut on Sepharose beads. Rat and goldfish clathrin both bound amph1-md mut, but the AP2 adaptor complex bound much more weakly ([Figure 4A](#)). The concentration of amph1-md mut that would be sufficient to sequester clathrin was assessed by using ITC to measure the affinity with which this domain bound the  $\beta$ -propeller of clathrin. The  $K_D$  was  $22 \pm 3 \mu M$  ([Figure 4B](#)), and the stoichiometry of the interaction was  $0.54 \pm 0.05$  (average of two independent measurements). These measurements suggest that two motif domains interact with one clathrin  $\beta$ -propeller, probably reflecting the presence of multiple protein interaction sites in the  $\beta$ -propeller and two sterically overlapping binding motifs in amph1-md mut ([Miele et al., 2004](#)).

Terminals were dialyzed with 0.1 mM amph1-md mut through the patch pipette. [Figure 4C](#) shows averaged capacitance responses elicited by depolarizations lasting 100 ms. Amph1-md mut inhibited the slow phase of endocytosis by a factor of 4 to 5 ( $k_{slow} = 0.02 \pm 0.008 s^{-1}$ ), leaving the fast phase unchanged in rate or amplitude ( $k_{fast} = 0.8 \pm 0.13 s^{-1}$  and  $A_{fast} = 59\% \pm 10\%$ ; [Table 1](#)). Amph1-md mut also slowed endocytosis after a stimulus lasting 2 s; ( $t_{1/2} > 30$  s compared to  $t_{1/2} = 10$  s in controls; [Figure 4D](#)). The sequestration of clathrin therefore selectively inhibited the slow phase of endocytosis. The fast phase of retrieval did not involve clathrin.

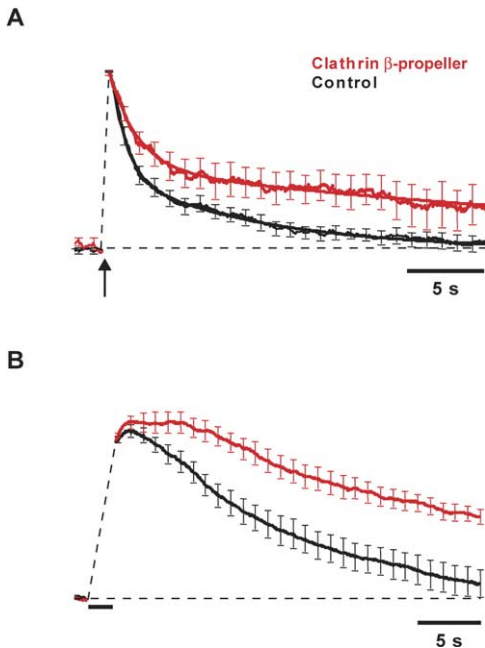


Figure 3. Inhibition of Slow Endocytosis by the  $\beta$ -Propeller Domain of Clathrin

(A) Normalized capacitance responses elicited by a depolarization lasting 100 ms (delivered at arrow). Averaged responses from terminals dialyzed with standard internal solution (black trace;  $n = 18$ ;  $\tau_{fast} = 1.1$  s and  $\tau_{slow} = 11.4$  s) or 0.1 mM clathrin  $\beta$ -propeller domain (red;  $n = 10$ ;  $\tau_{fast} = 1.9$  s and  $\tau_{slow} = 44$  s). (B) Normalized capacitance responses elicited by a depolarization lasting 2 s (delivered at bar). Averaged responses from terminals dialyzed with standard internal solution (black;  $n = 10$ ;  $t_{1/2} = 10 \pm 1.5$  s) or 0.1 mM clathrin  $\beta$ -propeller domain (red;  $n = 13$ ;  $t_{1/2} = 23.0 \pm 1$  s). The averaged amplitudes of the capacitance responses were as follows: standard internal solution,  $197 \pm 19$  fF; clathrin  $\beta$ -propeller,  $214 \pm 36$  fF. Error bars in graphs show  $\pm$  one SEM.

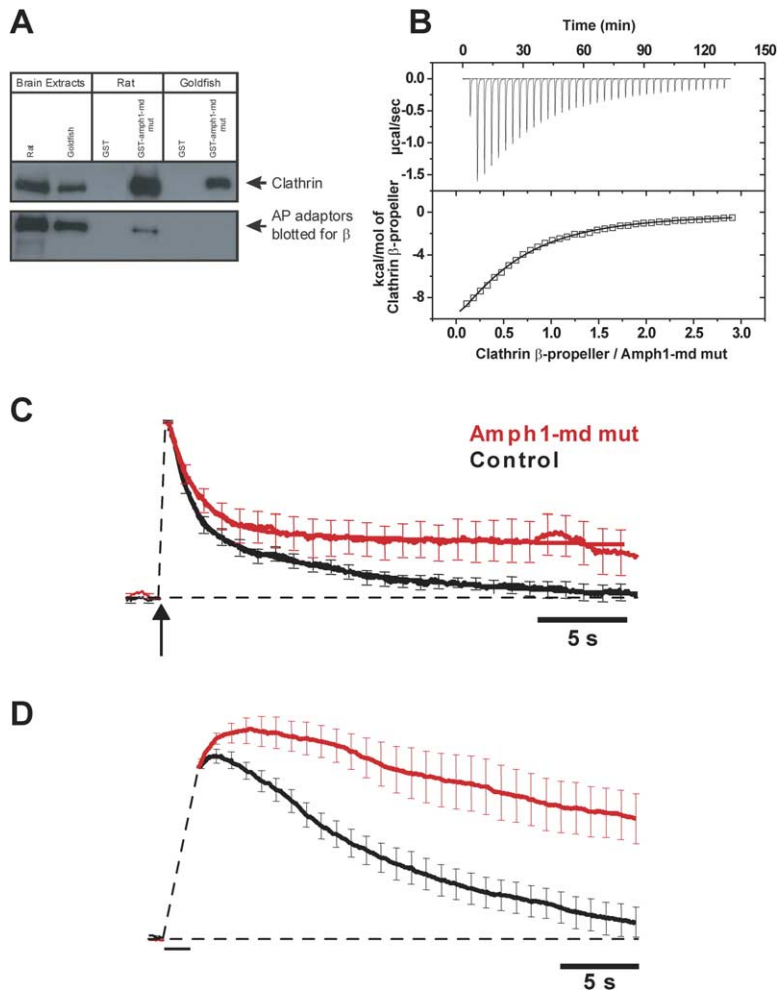


Figure 4. Sequestration of Clathrin Inhibited the Slow Phase of Endocytosis

(A) The interaction between GST-tagged rat amphiphysin 1 motif domain and rat or goldfish clathrin and AP2 adaptors was probed using a protein binding assay and followed by immunoblotting. The amphiphysin 1 motif domain covered residues 318–390 but had a mutation of DNF-DAF to reduce adaptor interactions (GST-amph1-md mut). (B) The interaction between amph1-md mut and rat clathrin  $\beta$ -propeller domain was followed by isothermal titration calorimetry. The upper panel shows the heat of binding measured by stepwise injection of 600  $\mu$ M clathrin  $\beta$ -propeller into 47  $\mu$ M amph1-md mut at 25°C. The lower panel shows the integrated heating powers of the upper panel normalized to the concentration of clathrin  $\beta$ -propeller domain. (C) Normalized capacitance responses elicited by a depolarization lasting 100 ms (delivered at arrow). Averaged responses from terminals dialyzed with standard internal solution (black trace;  $n = 18$ ;  $\tau_{fast} = 1.1$  s and  $\tau_{slow} = 11.4$  s) or 0.1 mM amph1-md mut (red;  $n = 10$ ;  $\tau_{fast} = 1.9$  and  $\tau_{slow} = 218$  s). (D) Normalized capacitance responses elicited by a depolarization lasting 2 s (delivered at bar). Averaged responses from terminals dialyzed with standard internal solution (black;  $n = 10$ ;  $t_{1/2} = 10$  s  $\pm$  1.5 s) or 0.1 mM amph1-md mut (red;  $n = 12$ ;  $t_{1/2} > 30$  s). The averaged amplitudes of the capacitance responses were as follows: standard internal solution, 197  $\pm$  19 fF; amph1-md mut, 308  $\pm$  38 fF. Error bars in graphs show  $\pm$  one SEM.

### The AP2 Adaptor Was Involved in Slow Endocytosis

Coated synaptic vesicles derived from mammalian brain are enriched in both clathrin and AP2 adaptors (Mills et al., 2003). We therefore also tested how AP2 was involved in endocytosis in the synaptic terminal of bipolar cells. The appendage domain of the  $\alpha$  subunit of the AP2 complex binds a number of accessory proteins (Owen et al., 1999), and a variety of different peptides can competitively inhibit these interactions (Praefcke et al., 2004). For instance, a 12mer containing the DNF motif of amphiphysin 1 binds the  $\alpha$  subunit of AP2 with especially high affinity ( $K_D$  of 2.5  $\mu$ M, as measured by ITC). Changing a single asparagine to proline reduces the affinity of the peptide; the  $K_D$  of the DPF-12mer was 120  $\mu$ M (Praefcke et al., 2004), allowing it to be used as a control. To test if a peptide derived from rat amphiphysin would inhibit the amphiphysin-AP2 interaction in goldfish, we performed a binding experiment using a GST-tagged construct of rat amphiphysin 1 containing the binding sites for the  $\alpha$  subunit of AP2 (amph1, residues 1–377). The western blots in Figure 5A show that amph1 (1–377) bound the AP2 adaptor complex from both rat and goldfish, but this binding was abolished by addition of 0.1 mM of the DNF-12mer.

Examples of individual capacitance responses elicited by depolarizations lasting 100 ms are shown in Figure 5B. In some terminals dialyzed with 0.1 mM of the DNF-12mer, only the fast phase of endocytosis could be observed, and a proportion of the excess membrane was not retrieved at all, i.e., the inhibition of the slow mode of endocytosis appeared complete. On average, the DNF-12mer inhibited the slow phase of endocytosis by a factor of 5 ( $k_{slow} = 0.02 \pm 0.011$  s $^{-1}$ ), leaving the fast phase unchanged ( $k_{fast} = 0.9 \pm 0.19$  s $^{-1}$ ; Figure 5C). The DPF-12mer, with a 50-fold lower affinity for the  $\alpha$  subunit of AP2, did not have any significant effect on fast or slow endocytosis (Figures 5B and 5C; Table 1). We conclude that the AP2 adaptor was involved in clathrin-mediated retrieval of synaptic vesicles in retinal bipolar cells and that this mechanism normally proceeds with a time constant of about 10 s. Equally, an interaction between the AP2 adaptor and amphiphysin was not involved in fast endocytosis.

### Fast Endocytosis Did Not Occur by a “Primed” Mechanism Dependent on Clathrin

A striking feature of the capacitance responses shown in Figures 5B and 5C is that a proportion of released vesicles could not be retrieved when the slow mode of

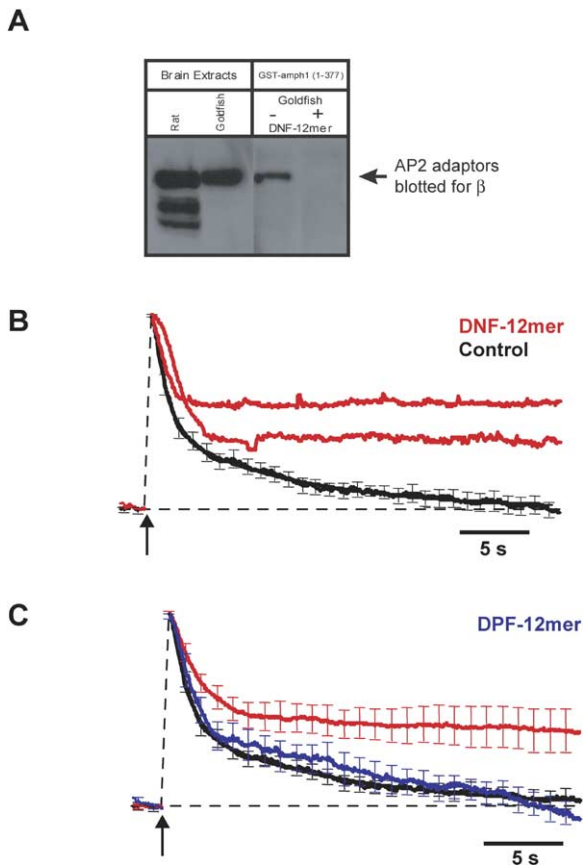


Figure 5. Adaptor Dependence of Slow Endocytosis

(A) The interaction of GST-tagged amphiphysin 1 (1–377) construct with the AP2 adaptor complex from goldfish brain and rat brain was probed by a binding assay and immunoblotting. This binding was abolished by the addition of an amphiphysin 1 peptide (DNF-12mer at 100  $\mu$ M final concentration). (B) Examples of capacitance responses elicited by a depolarization lasting 100 ms (delivered at arrow). Single responses from terminals dialyzed with standard internal solution (black), 0.1 mM DNF-12mer (red), and 0.1 mM DPF-12mer (blue). The responses are scaled to the same maximum to allow direct comparison. (C) Averaged scaled responses from terminals dialyzed with standard internal solution (black trace;  $n = 18$ ;  $\tau_{fast} = 1.1$  s and  $\tau_{slow} = 11.4$  s), 0.1 mM DNF-12mer (red;  $n = 7$ ;  $\tau_{fast} = 2.0$  and  $\tau_{slow} = 210$  s), and 0.1 mM DPF-12mer (blue;  $n = 13$ ;  $\tau_{fast} = 1.2$  and  $\tau_{slow} = 12.1$  s). Error bars in graphs show  $\pm$  one SEM.

endocytosis was inhibited. The fact that fast endocytosis did not compensate when slow endocytosis was blocked indicates that only a subset of released vesicles were capable of retrieval by the fast mechanism. Might this reflect a special population of vesicles “primed” for fast retrieval before fusion is triggered? Mueller et al. (2004) recently raised the possibility that fast and slow endocytosis in hippocampal boutons might both occur by a clathrin-dependent mechanism, with the fast mode reflecting a group of vesicles that become “primed” for fast retrieval. Such priming might occur by recruitment of adaptor and accessory proteins, or even preassembly of clathrin lattices. If this model applied to bipolar cells, peptides interfering with CME might be expected to inhibit the fast phase of retrieval only after repeated stimulation causing the re-

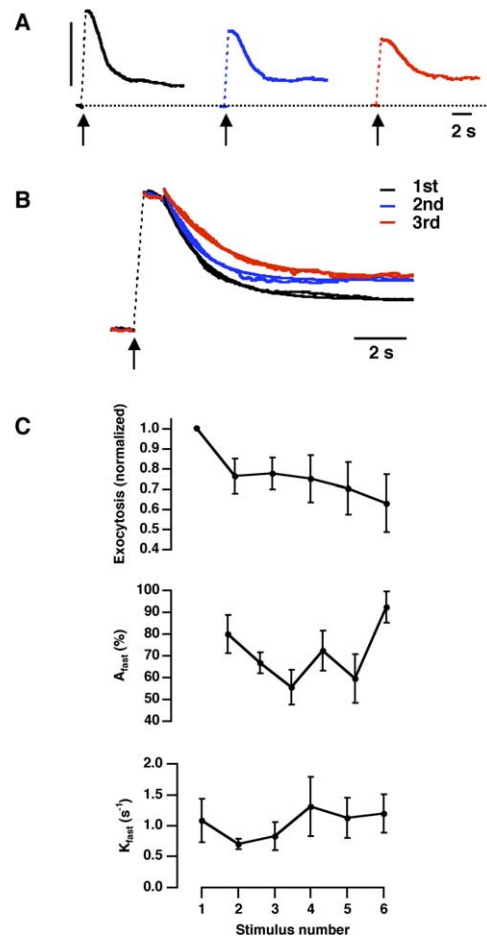


Figure 6. The Fast Phase of Endocytosis Was Still Apparent after Repeated Stimulation in the Presence of the DNF-12mer

(A) Three consecutive capacitance responses from a single terminal, which was dialyzed with internal solution containing 0.1 mM DNF-12mer and stimulated with 100 ms depolarizations delivered at 30 s intervals (delivered at arrows). (B) Responses from (A) scaled to the same maximum to allow direct comparison of the kinetics of endocytosis. The bold traces describing the time course of fast endocytosis are single exponentials declining with  $\tau$  ( $= 1/k_{fast}$ ) = 1.6 s for the first response,  $\tau = 1.3$  s for the second, and  $\tau = 2.1$  s for the third. (C) Averaged properties of capacitance responses during a train. Shown are the exocytic response normalized to the first stimulus (upper), the percentage of excess membrane retrieved during the fast phase (middle), and the rate constant of the fast phase (lower). The first four measurements are averages from seven cells, the fifth is from five cells, and the sixth is from three cells. Error bars show  $\pm$  one SEM.

lease of vesicles that were not primed at the time the peptide was introduced.

To test whether a population of vesicles were primed for CME, we monitored capacitance responses to repeated stimuli. Figure 6A shows a series of three consecutive responses to depolarizations lasting 100 ms delivered 36 s apart, all in the presence of 0.1 mM of the DNF-12mer. This duration stimulus completely depletes the rapidly releasable pool of vesicles (RRP; Mennerick and Matthews, 1996; Neves and Lagnado, 1999). In each case, the fast phase of retrieval was obvious, and

the slow phase was almost completely inhibited. These capacitance traces are shown normalized in Figure 6B, where the recovery phases have been fitted by single exponential functions. The fast phase of endocytosis occurred with rate constants of  $0.63\text{ s}^{-1}$ ,  $0.77\text{ s}^{-1}$ , and  $0.48\text{ s}^{-1}$ , all within the range normally observed (Neves et al., 2001; Neves and Lagnado, 1999). Averaged results are shown in Figure 6C, where it can be seen that the proportion of released vesicles retrieved by fast endocytosis, and the rate of this process, were relatively constant during repeated stimuli. We conclude that the fast phase of membrane retrieval did not represent a pool of vesicles primed for CME.

## Discussion

Real-time measurements have identified fast and slow modes of endocytosis at a number of synapses (Beutner et al., 2001; Gandhi and Stevens, 2003; Klingauf et al., 1998; Neves et al., 2001; Neves and Lagnado, 1999; Pyle et al., 2000; Sankaranarayanan and Ryan, 2000; Sun et al., 2002). The present study attempts to establish the molecular differences underlying these kinetically distinct mechanisms in retinal bipolar cells. The results indicate that the slow mode of endocytosis occurred through interactions of clathrin, AP2, and accessory proteins such as amphiphysin, while the fast mode of endocytosis did not involve any of these molecules (Figures 2–6).

### Fast and Slow Endocytosis Both Required GTP Hydrolysis

We found that fast and slow modes of endocytosis in bipolar cells were both dependent on the activity of a GTPase, since both were blocked when GTP in the internal solution was replaced by GTP- $\gamma$ -S or GDP- $\beta$ -S (Figure 1). The GTPase is most likely dynamin, given that slow retrieval was inhibited by a peptide blocking the binding of amphiphysin to dynamin (Figure 2; see also Yamashita et al., 2005) and the well-established role of dynamin in the recycling of synaptic vesicles in *Drosophila* (Koenig and Ikeda, 1989; van der Blik and Meyerowitz, 1991). The target of GTP- $\gamma$ -S was unlikely to be small G proteins, because these should be activated when bound to GTP- $\gamma$ -S. Although our observations contradict the recent suggestion that endocytosis in bipolar cells requires the hydrolysis of ATP rather than GTP (Heidelberger, 2001), they are in broad agreement with recent capacitance measurements of endocytosis in the calyx of Held, where a slow mode of endocytosis ( $\tau = 10\text{--}25\text{ s}$ ) also required GTP hydrolysis (Yamashita et al., 2005). If dynamin is also the GTPase involved in fast endocytosis in bipolar cells, it appears to be recruited by a protein other than amphiphysin, because disrupting the dynamin-amphiphysin interaction selectively inhibited the slow mode of retrieval (Figure 2).

### CME in Retinal Bipolar Cells

CME retrieves vesicle components in the correct proportions, because it involves the selection of the appropriate membrane cargo by the adaptor complex and generation of a vesicle of fixed size (Ford et al., 2001).

Clathrin and accessory proteins are enriched at synaptic terminals, including ribbon synapses of bipolar cells (Grabs et al., 2000; Hosoya and Tsutsui, 2004; Von Kriegstein et al., 1999; Yao et al., 2002; Sherry and Heidelberger, 2005). We identify CME as accounting for slow endocytosis in retinal bipolar cells (time constant  $\sim 10\text{ s}$ ), because the slow phase of membrane retrieval was selectively blocked by three different interventions: the  $\beta$ -propeller domain of clathrin that binds accessory proteins (Figure 3), the domain of amphiphysin 1 that binds clathrin (Figure 4), and the domain of amphiphysin 1 that binds the AP2 adaptor (Figure 5). Although clathrin-coated vesicles have not been regularly observed in electron micrographs of bipolar cell terminals (Holt et al., 2004; Paillart et al., 2003), we do not believe that this provides a strong argument against the existence of CME at this synapse. Clathrin and amphiphysin are enriched in the synaptic terminal of bipolar cells from the retina of goldfish (Sherry and Heidelberger, 2005), and clathrin-coated vesicles occur in abundance at the ribbon synapse of hair cells, which is structurally and functionally similar (Lenzi et al., 2002).

### Two Independent Pathways of Endocytosis

Two basic observations indicate that the fast and slow modes of endocytosis in bipolar cell terminals are substantially independent. First, brief stimuli that only release the RRP are followed almost exclusively by fast endocytosis, while slow retrieval becomes increasingly apparent after stronger stimuli that also release vesicles from the reserve pool (Neves et al., 2001; Neves and Lagnado, 1999). One possibility is that only the vesicles primed for fast exocytosis are capable of fast retrieval. This idea is supported by a second notable observation; blocking the slow mode of endocytosis completely prevented retrieval of a proportion of vesicles (Figures 5B and 6). In other words, the fast mode of retrieval could not substitute when the slow mode was blocked. The converse is not true, however. Fast endocytosis is inhibited by introduction of calcium buffers, when a proportion of vesicles from the RRP are retrieved by slow endocytosis instead of fast (Neves et al., 2001). Taken together, these results are consistent with the idea that fast retrieval operates on vesicles released from the RRP, while slower CME is an alternative default mechanism.

The ribbon synapses of hair cells and bipolar cells also support a mechanism of bulk membrane retrieval into large compartments, which can be observed after stimulation lasting tens of seconds (Holt et al., 2003; Lenzi et al., 2002; Paillart et al., 2003). Inhibitors of PI-3-kinase block bulk retrieval in bipolar cells, when endocytosis into small compartments takes over all membrane recycling (Holt et al., 2003). Notably, these inhibitors do not affect fast or slow phases of endocytosis observed in capacitance responses triggered by briefer stimuli (Holt et al., 2003). Bulk membrane retrieval is therefore quite distinct from the endocytic mechanisms that we have characterized in the present study.

### What Is the Mechanism of Fast Endocytosis?

The notion of fast endocytosis at the synapse is often taken to be synonymous with the term “kiss-and-run,”

a model of synaptic endocytosis that is distinguished by the idea that vesicles connect to the plasma membrane to release their contents without fully collapsing into the surface (Aravanis et al., 2003). One form of the “kiss-and-run” model proposes that the connection is a proteinaceous pore that opens to release the neurotransmitter and then rapidly closes before the vesicle is retrieved (Fesce et al., 1994; Klingauf et al., 1998; Richards et al., 2005). Zenisek et al. (2002) tested for “kiss-and-run” in retinal bipolar cells by using total internal reflection fluorescence microscopy (TIRF) to visualize directly fusion of individual vesicles labeled with FM1-43 and the subsequent diffusion of the dye in the surface of the synaptic terminal. Fusion was always followed by complete loss of FM1-43 from the vesicle, indicating free exchange of lipids between the vesicle and the plasma membrane. Llobet et al. (2003) tested for “kiss-and-run” in bipolar cells using a different approach; instead of looking for partial loss of vesicle contents, they investigated whether vesicles collapse by directly monitoring expansion of the surface membrane using interference reflection microscopy (IRM). Brief stimuli caused vesicles to merge into the surface, and this excess membrane was retracted with a time constant of 1 s, reflecting fast endocytosis. The results of TIRF and IRM therefore argue strongly against “kiss-and-run” as an important mechanism of exocytosis in bipolar cells.

CME is a relatively complex process, requiring the sequential recruitment of a large number of proteins to coat a single vesicle (Praefcke et al., 2004). Here, we have measured the speed of CME as about 10 s, and this may reflect a limit for the rate at which these components can be supplied by diffusion and subsequently assembled before membrane scission by dynamin. Perhaps the fast mode of endocytosis reflects the use of fewer molecules arranged in less precise patterns. This process does not appear to involve the AP2 adaptor complex (Figure 5) or accessory proteins that contain a clathrin binding motif, such as amphiphysin (Figure 3), although it seems likely that the final scission step is also mediated by dynamin. We therefore suggest that fast endocytosis in the synaptic terminal of retinal bipolar cells occurs by the retrieval of membrane that has collapsed into the surface, but *without* formation of a clathrin coat. It will be interesting to determine whether fast retrieval of surface membrane by a clathrin-independent mechanism occurs at other synapses. Which molecules are involved in fast endocytosis?

## Experimental Procedures

### Electrophysiology

Depolarizing bipolar cells were acutely dissociated from the retinas of goldfish using methods described previously (Lagnado et al., 1996). The normal Ringer's solution contained the following: 120 mM NaCl, 2.5 mM KCl, 1 mM MgCl<sub>2</sub>, 2.5 mM CaCl<sub>2</sub>, 10 mM glucose, 10 mM HEPES (pH 7.3, 280 mOsm/kg). Capacitance measurements were made from synaptic terminals that had detached from the axon during dissociation using methods described by Neves and Lagnado (1999). Unless otherwise stated, the solution in the patch pipette contained the following: 110 mM cesium methanesulfonate, 5 mM MgCl<sub>2</sub>, 3 mM Na<sub>2</sub>ATP, 1 mM Na<sub>2</sub>GTP, 10 mM TEA-Cl, 0.4 mM BAPTA, and 20 mM HEPES (pH 7.2, 260 mOsm/kg).

Electrode resistances were 4–7 M $\Omega$ ; the input resistance of the terminals was typically 1–10 G $\Omega$  at the holding potential of  $-70$  mV. All depolarizing voltage steps were to  $-10$  mV.

Peptides and protein domains to be introduced into the terminal were dissolved in standard internal solution. Aliquots of peptide solutions were made at a concentration of 1.0 mM or 5 mM and stored at  $-20^{\circ}\text{C}$ . If necessary, the pH of the solution was adjusted back to 7.2 before freezing. Protein domains were purified as described below and stored at  $-80^{\circ}\text{C}$ . On the day of use, one aliquot was thawed and diluted with the standard internal solution to the desired concentration.

### Fitting of Capacitance Traces and Statistics

Visual inspection of capacitance records indicated that the fall in membrane surface area usually occurred as two phases. A useful way to compare measurements made under different conditions, therefore, was to fit double exponential functions using the fitting procedure in IGOR PRO software (WaveMetrics, Lake Oswego, OR), as described by Neves and Lagnado (1999). The collected results in Table 1 were obtained by fitting a number of individual traces under each condition, then calculating the mean and standard error of the mean. In some records (e.g., Figure 5B), the second phase of retrieval appeared to be absent, and it was not possible to make a reliable estimate of the rate constant for slow endocytosis ( $k_{\text{slow}}$ ), in which case a value of zero was recorded for the purpose of collecting statistics. Occasionally, the amplitude of the slow phase was very small relative to the fast phase, again making an estimate of the rate constant unreliable. In such situations, the trace was fit with a single exponential to estimate  $k_{\text{fast}}$ , and the amplitude of the slow phase was recorded as zero.

Averaged traces shown in the figures were obtained by first normalizing all the records under a particular condition, then calculating the mean and standard deviation on a point-by-point basis. Best-fit curves were calculated, taking into account the standard deviation. When fitting averaged traces, it was always possible to obtain reliable descriptions using a double exponential function. For this reason, the values of the parameters for the best-fit curves (see figure legends) were slightly different from values obtained by compiling measurements from individual traces (Table 1). Values are given as mean  $\pm$  SEM.

### Recombinant Proteins

Rat amphiphysin 1 (residues 1–390) and bovine clathrin  $\beta$ -propeller domain (residues 1–363) were subcloned into pGEX4T2, expressed in *E. coli* BL21 cells, purified by glutathione-affinity, cleaved with thrombin, and further purified by ion exchange chromatography and gel filtration before use.

### Preparation of Brain Lysates

To prepare brain lysate, one rat brain or four goldfish brains were put into a glass homogenizer (Bio-Rad) with 5 ml of a solution containing 20 mM HEPES (pH 7.4), 150 mM NaCl, 1 mM DTT, 0.1% Triton, and 0.1% protease inhibitors (Sigma). The brains were then homogenized for several minutes at  $4^{\circ}\text{C}$ . The homogenate was spun down for 25 min at 50,000 rpm at  $4^{\circ}\text{C}$  and either used immediately or frozen in liquid nitrogen and stored at  $-80^{\circ}\text{C}$ .

### Protein Binding Assays

Recombinant proteins were purified as above without thrombin cleavage. The amount of bead bound protein was estimated by Coomassie staining after PAGE.

For a single protein binding assay, 0.5 ml of brain lysate was added to 20  $\mu\text{g}$  of bead bound protein, using the estimate from the Coomassie analysis, and incubated for 1 hr at  $4^{\circ}\text{C}$  on a rotator. After the incubation, the beads were spun down and washed very carefully three times with 20 mM HEPES (pH 7.4), 150 mM NaCl, 1 mM DTT, and 0.1% protease inhibitors and twice with 20 mM HEPES (pH 7.4), 150 mM NaCl, and 1 mM DTT. Then, 60  $\mu\text{l}$  sample buffer was added to the beads, and the samples were boiled for 3 min at  $80^{\circ}\text{C}$ . Afterward, 5  $\mu\text{l}$  of the samples was resolved by SDS-PAGE. As a reference, a small aliquot of the brain extract was run on the same gel. The proteins were then transferred to nitrocellu-



lose by Western blotting to confirm binding of proteins to the recombinant bead bound proteins.

#### ITC

ITC was performed using a VP-ITC (Microcal). All titrations were performed using purified protein in 50 mM HEPES (pH 7.4), 120 mM NaCl, and 1 mM DTT at 25°C or 10°C. Ligands were made up in thoroughly de-aerated buffer and were injected into the experimental cell containing the protein solution. Ligand was injected into the cell in ~40 small steps (usually 7  $\mu$ l per step), until there was a molar excess of ligand within the cell. After each individual injection, the released heat of binding was recorded for 3.5 min. The protein concentration used within the cell was three to five times that of the expected affinity, based on previously published data or estimates from our sedimentation assays. Protein concentrations in the range of 40–250  $\mu$ M were therefore common. Control experiments, where ligand was injected into de-aerated buffer, were also performed, and results were subtracted from the experimental data to control for heat of dilution. All results were analyzed using the ORIGIN software package (Microcal). The curve fit to the data describes a single site binding model:  $dq/dLt = \Delta H (1/2 + (1 - XR - r)/(2((XR + r + 1)^2 - 4XR)1/2)) V$ , with  $XR = [L_T]/[M_T]$  and  $r = 1/K_A[M_T]$  (Wiseman et al., 1989). For a full derivation of this equation, see Indyk and Fisher (1998). This fit optimizes parameters of stoichiometry (N), association constant ( $K_A$ ), and the enthalpy of binding ( $\Delta H$ ). The dissociation constant ( $K_D$ ) is the inverse of  $K_A$ . For display purposes, the integrated data were shown normalized to the concentration of injected ligand.

#### Acknowledgments

We thank our coworkers in the Lagnado and McMahon labs for many useful discussions. This work was supported by the Medical Research Council and the Human Frontiers in Science Program (grant to L.L.).

Received: August 23, 2004

Revised: March 3, 2005

Accepted: May 2, 2005

Published: June 15, 2005

#### References

- Aravanis, A.M., Pyle, J.L., and Tsien, R.W. (2003). Single synaptic vesicles fusing transiently and successively without loss of identity. *Nature* 423, 643–647.
- Beutner, D., Voets, T., Neher, E., and Moser, T. (2001). Calcium dependence of exocytosis and endocytosis at the cochlear inner hair cell afferent synapse. *Neuron* 29, 681–690.
- Bloom, G.S., Richards, B.W., Leopold, P.L., Ritchey, D.M., and Brady, S.T. (1993). GTP gamma S inhibits organelle transport along axonal microtubules. *J. Cell Biol.* 120, 467–476.
- Ceccarelli, B., Hurlbut, W.P., and Mauro, A. (1973). Turnover of transmitter and synaptic vesicles at the frog neuromuscular junction. *J. Cell Biol.* 57, 499–524.
- Cremona, O., and De Camilli, P. (1997). Synaptic vesicle endocytosis. *Curr. Opin. Neurobiol.* 7, 323–330.
- David, C., McPherson, P.S., Mundigl, O., and de Camilli, P. (1996). A role of amphiphysin in synaptic vesicle endocytosis suggested by its binding to dynamin in nerve terminals. *Proc. Natl. Acad. Sci. USA* 93, 331–335.
- Dell'Angelica, E.C., Klumperman, J., Stoorvogel, W., and Bonifacino, J.S. (1998). Association of the AP-3 adaptor complex with clathrin. *Science* 280, 431–434.
- Fesce, R., Grohovaz, F., Valtorta, F., and Meldolesi, J. (1994). Neurotransmitter release: fusion or 'kiss-and-run'? *Trends Cell Biol.* 4, 1–4.
- Ford, M.G., Pearse, B.M., Higgins, M.K., Vallis, Y., Owen, D.J., Gibson, A., Hopkins, C.R., Evans, P.R., and McMahon, H.T. (2001). Simultaneous binding of PtdIns(4,5)P<sub>2</sub> and clathrin by AP180 in the

nucleation of clathrin lattices on membranes. *Science* 291, 1051–1055.

- Gandhi, S.P., and Stevens, C.F. (2003). Three modes of synaptic vesicular recycling revealed by single-vesicle imaging. *Nature* 423, 607–613.
- Grabs, D., Slepnev, V.I., Songyang, Z., David, C., Lynch, M., Cantley, L.C., and De Camilli, P. (1997). The SH3 domain of amphiphysin binds the proline-rich domain of dynamin at a single site that defines a new SH3 binding consensus sequence. *J. Biol. Chem.* 272, 13419–13425.
- Grabs, D., Bergmann, M., and Rager, G. (2000). Developmental expression of amphiphysin in the retinotectal system of the chick: from mRNA to protein. *Eur. J. Neurosci.* 12, 1545–1553.
- Heidelberger, R. (2001). ATP is required at an early step in compensatory endocytosis in synaptic terminals. *J. Neurosci.* 21, 6467–6474.
- Heuser, J.E., and Reese, T.S. (1973). Evidence for recycling of synaptic vesicle membrane during transmitter release at the frog neuromuscular junction. *J. Cell Biol.* 57, 315–344.
- Holt, M., Cooke, A., Wu, M.M., and Lagnado, L. (2003). Bulk membrane retrieval in the synaptic terminal of retinal bipolar cells. *J. Neurosci.* 23, 1329–1339.
- Holt, M., Cooke, A., Neef, A., and Lagnado, L. (2004). High mobility of vesicles supports continuous exocytosis at a ribbon synapse. *Curr. Biol.* 14, 173–183.
- Hosoya, O., and Tsutsui, K. (2004). Localized expression of amphiphysin I<sub>r</sub>, a retina-specific variant of amphiphysin I, in the ribbon synapse and its functional implication. *Eur. J. Neurosci.* 19, 2179–2187.
- Hull, C., and von Gersdorff, H. (2004). Fast endocytosis is inhibited by GABA-mediated chloride influx at a presynaptic terminal. *Neuron* 44, 469–482.
- Indyk, L., and Fisher, H.F. (1998). Theoretical aspects of isothermal titration calorimetry. *Methods Enzymol.* 295, 350–364.
- Jarousse, N., and Kelly, R.B. (2001). Endocytotic mechanisms in synapses. *Curr. Opin. Cell Biol.* 13, 461–469.
- Klingauf, J., Kavalali, E.T., and Tsien, R.W. (1998). Kinetics and regulation of fast endocytosis at hippocampal synapses. *Nature* 394, 581–585.
- Koenig, J.H., and Ikeda, K. (1989). Disappearance and reformation of synaptic vesicle membrane upon transmitter release observed under reversible blockage of membrane retrieval. *J. Neurosci.* 9, 3844–3860.
- Krupnick, J.G., Goodman, O.B., Jr., Keen, J.H., and Benovic, J.L. (1997). Arrestin/clathrin interaction. Localization of the clathrin binding domain of nonvisual arrestins to the carboxy terminus. *J. Biol. Chem.* 272, 15011–15016.
- Lagnado, L., Gomis, A., and Job, C. (1996). Continuous vesicle cycling in the synaptic terminal of retinal bipolar cells. *Neuron* 17, 957–967.
- Lenzi, D., Crum, J., Ellisman, M.H., and Roberts, W.M. (2002). Depolarization redistributes synaptic membrane and creates a gradient of vesicles on the synaptic body at a ribbon synapse. *Neuron* 36, 649–659.
- Llobet, A., Beaumont, V., and Lagnado, L. (2003). Real-time measurement of exocytosis and endocytosis using interference of light. *Neuron* 40, 1075–1086.
- Marks, B., Stowell, M.H., Vallis, Y., Mills, I.G., Gibson, A., Hopkins, C.R., and McMahon, H.T. (2001). GTPase activity of dynamin and resulting conformation change are essential for endocytosis. *Nature* 410, 231–235.
- Marsh, M., and McMahon, H.T. (1999). The structural era of endocytosis. *Science* 285, 215–220.
- Mennerick, S., and Matthews, G. (1996). Ultrafast exocytosis elicited by calcium current in synaptic terminals of retinal bipolar neurons. *Neuron* 17, 1241–1249.
- Miele, A.E., Watson, P.J., Evans, P.R., Traub, L.M., and Owen, D.J. (2004). Two distinct interaction motifs in amphiphysin bind two in-

- dependent sites on the clathrin terminal domain  $\beta$ -propeller. *Nat. Struct. Mol. Biol.* **11**, 242–248.
- Mills, I.G., Praefcke, G.J., Vallis, Y., Peter, B.J., Olesen, L.E., Gallop, J.L., Butler, P.J., Evans, P.R., and McMahon, H.T. (2003). EpsinR: an AP1/clathrin interacting protein involved in vesicle trafficking. *J. Cell Biol.* **160**, 213–222.
- Morgan, J.R., Augustine, G.J., and Lafer, E.M. (2002). Synaptic vesicle endocytosis: the races, places, and molecular faces. *Neuromolecular Med.* **2**, 101–114.
- Mueller, V.J., Wienisch, M., Nehring, R.B., and Klingauf, J. (2004). Monitoring clathrin-mediated endocytosis during synaptic activity. *J. Neurosci.* **24**, 2004–2012.
- Neves, G., and Lagnado, L. (1999). The kinetics of exocytosis and endocytosis in the synaptic terminal of goldfish retinal bipolar cells. *J. Physiol.* **515**, 181–202.
- Neves, G., Gomis, A., and Lagnado, L. (2001). Calcium influx selects the fast mode of endocytosis in the synaptic terminal of retinal bipolar cells. *Proc. Natl. Acad. Sci. USA* **98**, 15282–15287.
- Owen, D.J., Wigge, P., Vallis, Y., Moore, J.D., Evans, P.R., and McMahon, H.T. (1998). Crystal structure of the amphiphysin-2 SH3 domain and its role in the prevention of dynamin ring formation. *EMBO J.* **17**, 5273–5285.
- Owen, D.J., Vallis, Y., Noble, M.E., Hunter, J.B., Dafforn, T.R., Evans, P.R., and McMahon, H.T. (1999). A structural explanation for the binding of multiple ligands by the alpha-adaptin appendage domain. *Cell* **97**, 805–815.
- Paillart, C., Li, J., Matthews, G., and Sterling, P. (2003). Endocytosis and vesicle recycling at a ribbon synapse. *J. Neurosci.* **23**, 4092–4099.
- Praefcke, G.J., and McMahon, H.T. (2004). The dynamin superfamily: universal membrane tubulation and fission molecules? *Nat. Rev. Mol. Cell Biol.* **5**, 133–147.
- Praefcke, G.J., Ford, M.G., Schmid, E.M., Olesen, L.E., Gallop, J.L., Peak-Chew, S.Y., Vallis, Y., Babu, M.M., Mills, I.G., and McMahon, H.T. (2004). Evolving nature of the AP2  $\alpha$ -appendage hub during clathrin-coated vesicle endocytosis. *EMBO J.* **23**, 4371–4383.
- Pyle, J.L., Kavalali, E.T., Piedras-Renteria, E.S., and Tsien, R.W. (2000). Rapid reuse of readily releasable pool vesicles at hippocampal synapses. *Neuron* **28**, 221–231.
- Ramjaun, A.R., and McPherson, P.S. (1998). Multiple amphiphysin II splice variants display differential clathrin binding: identification of two distinct clathrin-binding sites. *J. Neurochem.* **70**, 2369–2376.
- Richards, D.A., Bai, J., and Chapman, E.R. (2005). Two modes of exocytosis at hippocampal synapses revealed by rate of FM1-43 efflux from individual vesicles. *J. Cell Biol.* **168**, 929–939.
- Royle, S.J., and Lagnado, L. (2003). Endocytosis at the synaptic terminal. *J. Physiol.* **553**, 345–355.
- Sankaranarayanan, S., and Ryan, T.A. (2000). Real-time measurements of vesicle-SNARE recycling in synapses of the central nervous system. *Nat. Cell Biol.* **2**, 197–204.
- Schmid, S.L., McNiven, M.A., and De Camilli, P. (1998). Dynamin and its partners: a progress report. *Curr. Opin. Cell Biol.* **10**, 504–512.
- Sherry, D.M., and Heidelberger, R. (2005). Distribution of proteins associated with synaptic vesicle endocytosis in the mouse and goldfish retina. *J. Comp. Neurol.* **484**, 440–457.
- Shupliakov, O., Low, P., Grabs, D., Gad, H., Chen, H., David, C., Takei, K., De Camilli, P., and Brodin, L. (1997). Synaptic vesicle endocytosis impaired by disruption of dynamin-SH3 domain interactions. *Science* **276**, 259–263.
- Sun, J.Y., Wu, X.S., and Wu, L.G. (2002). Single and multiple vesicle fusion induce different rates of endocytosis at a central synapse. *Nature* **417**, 555–559.
- Sweitzer, S.M., and Hinshaw, J.E. (1998). Dynamin undergoes a GTP-dependent conformational change causing vesiculation. *Cell* **93**, 1021–1029.
- van der Bliek, A.M., and Meyerowitz, E.M. (1991). Dynamin-like protein encoded by the *Drosophila shibire* gene associated with vesicular traffic. *Nature* **351**, 411–414.
- von Gersdorff, H., and Matthews, G. (1994). Dynamics of synaptic vesicle fusion and membrane retrieval in synaptic terminals. *Nature* **367**, 735–739.
- Von Kriegstein, K., Schmitz, F., Link, E., and Sudhof, T.C. (1999). Distribution of synaptic vesicle proteins in the mammalian retina identifies obligatory and facultative components of ribbon synapses. *Eur. J. Neurosci.* **11**, 1335–1348.
- Wigge, P., Kohler, K., Vallis, Y., Doyle, C.A., Owen, D., Hunt, S.P., and McMahon, H.T. (1997). Amphiphysin heterodimers: potential role in clathrin-mediated endocytosis. *Mol. Biol. Cell* **8**, 2003–2015.
- Wiseman, T., Williston, S., Brandts, J.F., and Lin, L.N. (1989). Rapid measurement of binding constants and heats of binding using a new titration calorimeter. *Anal. Biochem.* **179**, 131–137.
- Yamashita, T., Hige, T., and Takahashi, T. (2005). Vesicle endocytosis requires dynamin-dependent GTP hydrolysis at a fast CNS synapse. *Science* **307**, 124–127.
- Yao, P.J., Coleman, P.D., and Calkins, D.J. (2002). High-resolution localization of clathrin assembly protein AP180 in the presynaptic terminals of mammalian neurons. *J. Comp. Neurol.* **447**, 152–162.
- Zenisek, D., Steyer, J.A., Feldman, M.E., and Almers, W. (2002). A membrane marker leaves synaptic vesicles in milliseconds after exocytosis in retinal bipolar cells. *Neuron* **35**, 1085–1097.